NeuroImage 251 (2022) 119001

Contents lists available at ScienceDirect

NeuroImage

journal homepage: www.elsevier.com/locate/neuroimage

Resolution of diaschisis contributes to early recovery from post-stroke aphasia

Max Wawrzyniak[a,*], Hans R. Schneider[a], Julian Klingbeil[a], Anika Stockert[a], Gesa Hartwigsen[b], Cornelius Weiller[c], Dorothee Saur[a]

[a] Language and Aphasia Laboratory, Department of Neurology, University of Leipzig Medical Center, Leipzig, Germany
[b] Lise Meitner Research Group 'Cognition and Plasticity', Max Planck Institute for Human Cognitive and Brain Sciences, Leipzig, Germany
[c] Freiburg Brain Imaging Center, Department of Neurology, University of Freiburg, Freiburg, Germany

ARTICLE INFO

Keywords:
Aphasia
Stroke
Recovery
Diaschisis
Connectivity
fMRI

ABSTRACT

Diaschisis is a phenomenon observed in stroke that is defined as neuronal dysfunction in regions spared by the infarction but connected to the lesion site.

We combined lesion network mapping and task-based functional MRI in 71 patients with post-stroke aphasia to investigate, whether diaschisis and its resolution contribute to early loss and recovery of language functions. Language activation acquired in the acute, subacute and chronic phase was analyzed in compartments with high and low normative resting-state functional connectivity to the lesion site on an individual basis.

Regions with high compared to regions with low lesion connectivity showed a steeper increase in language reactivation from the acute to the subacute phase. This finding is compatible with the assumption of resolution of diaschisis. Additionally, language performance in the subacute phase and improvement from the subacute to the chronic phase significantly correlated with the diaschisis effect and its resolution, respectively, suggesting a behavioral relevance of this effect.

We therefore assume that undamaged but functionally connected regions become dysfunctional due to missing input from the lesion contributing to the aphasic deficit. Since these regions are structurally intact, dysfunction resolves over time contributing to the rapid early behavioral improvement observed in aphasic stroke patients. Our results demonstrate that diaschisis and its resolution might be a relevant mechanism of early loss and recovery of language function in acute stroke patients.

1. Introduction

Approximately one third of all stroke patients present with initial aphasia (Engelter et al., 2006; Laska et al., 2001; Lazar et al., 2008; Pedersen et al., 1995). The natural course of recovery is typically characterized by a rapid early language improvement followed by a much slower recovery over months and years (Hillis and Heidler, 2002; Laska et al., 2011; Stockert et al., 2016), while some patients continue to improve even years after stroke (Holland et al., 2017; Hope et al., 2017). There is no fix boundary between these early and late phases and recovery is also dependent on therapeutic interventions. However, the rapid early improvement is mainly observed within the first days to weeks after stroke (Laska et al., 2011; Pedersen et al., 1995).

Several neuronal mechanisms have been suggested to underlie language recovery after stroke. These include reorganization of the residual language network in the left hemisphere (Saur et al., 2006; Stockert et al., 2020; Weiller et al., 1995), recruitment of contralesional cortex (Stockert et al., 2020; Weiller et al., 1995; Xing et al., 2016) and compensation by domain-general networks (Brownsett et al., 2014; Geranmayeh et al., 2014). However, these mechanisms seem to be relevant mainly in the subacute and chronic phase after stroke. Two fundamentally different mechanisms might be of importance for loss and recovery of function in the early phase post stroke. The first is reperfusion of the ischemic penumbra (Hillis et al., 2008; Hossmann, 1994). The second is the phenomenon of diaschisis and its resolution. The term diaschisis refers to a temporary neuronal dysfunction with associated neurological deficits in regions spared by the stroke but normally connected to the lesion site (von Monakow, 1914). Diaschisis begins simultaneously with stroke onset and typically resolves over time accompanied by some amount of early functional improvement (Carrera and Tononi, 2014). Perfusion and electrophysiological correlates of diaschisis in terms of lesion-remote dysfunction have been demonstrated

Abbreviations: LRS, Language recovery score; Rev, unintelligible reversed speech; Sp, intelligible speech.

* Corresponding author at: Klinik und Poliklinik für Neurologie, Universitätsklinikum Leipzig AöR, Liebigstraße 20, 04103 Leipzig, Germany.
E-mail address: max.wawrzyniak@medizin.uni-leipzig.de (M. Wawrzyniak).

https://doi.org/10.1016/j.neuroimage.2022.119001.
Received 9 April 2021; Received in revised form 31 January 2022; Accepted 12 February 2022
Available online 13 February 2022.

previously (Corbetta et al., 2005; DeMarco and Turkeltaub, 2020; Grefkes et al., 2008; He et al., 2007; Kim et al., 2012). However, the contribution to loss and recovery of functions remains incompletely understood (Carrera and Tononi, 2014).

Recent methodological advances in the study of diaschisis have been made by Boes et al. (2015) who presented a new approach termed lesion network mapping. Functional networks potentially affected by the stroke lesion were identified using normative functional connectome data from large-scale resting-state fMRI data sets of healthy participants. The lesion site is used as a seed for a functional connectivity analysis under the assumption that regions with high normative functional connectivity to the lesion are most vulnerable to diaschisis (Fox, 2018). Importantly, besides the individual lesion location, this approach requires no additional specialized imaging, since connectome data from healthy participants is used to identify regions (formerly) connected to the lesion. Also, while classic lesion-behavior mapping is only informative in regions with substantial lesion overlap, lesion network mapping is suitable given widespread lesion locations and is informative in any region potentially connected to lesions associated with the symptom of interest. Using this technique, anatomical correlates of various neurological symptoms arising from distributed lesion locations could be identified (Boes et al., 2015; Fox, 2018; Klingbeil et al., 2020; Wawrzyniak et al., 2018). This technique was also applied to a group of 12 patients with non-fluent aphasia due to subcortical hemorrhage. Notably, lesion networks of all patients overlapped in Broca's region suggesting diaschisis effects in Broca's area as a possible cause for aphasia in these patients (Boes et al., 2015). However, the contribution of diaschisis effects to aphasia due to subcortical lesions remains a matter of debate (Boes et al., 2015; Hillis et al., 2002; Kim et al., 2012; Nadeau and Crosson, 1997; Perani et al., 1987; Sebastian et al., 2014; Wallesch et al., 1997; Weiller et al., 1993).

Even less is known about the role of diaschisis in the typical case of aphasia caused by cortical lesions. Previous functional neuroimaging studies revealed a global breakdown of language activation in the acute phase post stroke which then resolves over weeks (Saur et al., 2006) to months (Cappa et al., 1997). Subsequent reactivation of the residual language network has been demonstrated to be associated with behavioral improvement (Cappa et al., 1997; Saur et al., 2006; Stockert et al., 2020). Nevertheless, it remains an open question whether resolution of diaschisis is the underlying mechanism that drives reactivation in the language network with concomitant early language recovery in these patients.

In the present study, we used a novel combination of lesion network mapping based on normative resting-state functional MRI data and longitudinal language fMRI in a large cohort of stroke patients with aphasia mostly due to cortical infarcts. To identify regions that are potentially affected by diaschisis, we analyzed language fMRI activation acquired in the acute, subacute and chronic phase in individually defined compartments with high and low functional resting-state connectivity to the lesion. We hypothesize that resolution of the acute breakdown in fMRI language activation depends on connectivity to the lesion site and is behaviorally relevant for early language recovery.

2. Material and methods

All experimental procedures were approved by the local ethics committees according to the Declaration of Helsinki. Written informed consent was given by each participant or her/his legal guardian.

For a methodological overview, see Fig. 1. In short, to operationalize diaschisis, we calculated functional connectivity of each individual lesion to all other parts of the brain using resting-state fMRI scans from an age and sex matched normative cohort (i.e. normative lesion connectivity). A predefined mask, representing regions with potential diaschisis effects, was then divided into compartments with high and low normative lesion connectivity on an individual basis. We expected diaschisis effects especially in brain regions with high connectivity to the lesion. Regions with low connectivity to the lesion served as a baseline to control for other effects like reperfusion or underactivation due to poor task performance. From these individual regions with high and low lesion connectivity, we extracted the mean fMRI effect size for intelligible > unintelligible speech for all available measurements which were subsequently fed into a repeated measures analysis of variance (rmANOVA) with the factors lesion connectivity (high, low) and time (acute, subacute, chronic).

2.1. Patients and healthy controls

We analyzed data from 71 right-handed patients (age 58.0 ± 14.0; 69.0% male) with acute aphasia confirmed by formal testing due to first-ever left-hemispheric ischemic stroke taken from previous studies from our laboratory (Saur et al., 2010, 2006; Stockert et al., 2020). Patients were enrolled at the university hospitals of Hamburg (05/2003 – 12/2004; $n = 13$), Freiburg (06/2006 – 03/2010; $n = 51$) and Leipzig (06/2011 – 05/2014; $n = 7$), Germany (Supplementary Table 1). Exclusion criteria were persisting large intracranial vessel occlusion at the time of first fMRI examined by transcranial color-coded duplex sonography, severe small vessel disease, large vessel disease with hemodynamic infarctions, seizures, tumors, reduced general health status, preexisting neuropsychological impairments (e.g., dementia), native language other than German, severe hearing deficits, contraindications for MRI and incomplete/corrupt data sets due to technical or compliance problems. See Supplementary Tables 1 and 2 for detailed demographic information and language testing results and Fig. 2 for a lesion overlay. Additionally, we selected 14 healthy age- and sex-matched controls (age 57.6 ± 13.6; 57.1% male) from our database. All patients were examined longitudinally up to three times: In the acute (day 0 – 3; $\varnothing = 1.8$; $n = 55$), subacute (day 4 – 22; $\varnothing = 10.7$; $n = 69$) and chronic (day 84 – 696; $\varnothing = 150.0$; $n = 53$) phase after stroke, while controls were examined once. The definition of phases largely differs between studies in the field. Comparisons with other studies should therefore be made cautiously.

2.2. Magnetic resonance imaging

We used functional MRI to quantify language specific blood-oxygenation level dependent (BOLD) signal in the brain in all patients and healthy controls. Short German sentences (1.7 – 2.7 s) were presented under two conditions: Intelligible speech with or without a semantic violation (e.g., 'The pilot flies/eats the plane.', hence termed 'Sp') and unintelligible temporally reversed speech (e.g., '.enalp eht stae/seilf tolip ehT', hence termed 'Rev'). Stimulus presentation was performed with the software Presentation (Neurobehavioral Systems, Inc., USA, https://www.neurobs.com) in an event-related design. The actual fMRI paradigms slightly varied between the three research sites. In paradigm I, 92 stimuli in each condition (Sp and Rev) were evenly distributed over 6 sessions (Saur et al., 2006; Stockert et al., 2020). In paradigm II, 90 stimuli per condition were distributed over 3 sessions for the controls while patients only completed one single session with 30 stimuli per condition (Saur et al., 2008; Stockert et al., 2020). Participants were asked to press a button with their left index finger (i) whenever a sentence was incorrect or reverse played (paradigm I) or (ii) following each stimulus (paradigm II). See Supplementary Table 2 for individual in-scanner performance data. Note, that all analyses in this paper are based on extensive language testing performed outside the scanner (see next section). Patients and controls examined in Hamburg and Leipzig and 11 patients examined in Freiburg underwent paradigm I; all other patients and all controls examined in Freiburg underwent paradigm II (Supplementary Table 1).

MRI was performed at 3 Tesla scanners (Siemens Trio in Hamburg/Freiburg and Siemens Verio in Leipzig). Functional imaging comprised whole brain images acquired using an echo planar imaging (EPI) sequence (Hamburg: 115 scans per session, repetition time (TR):

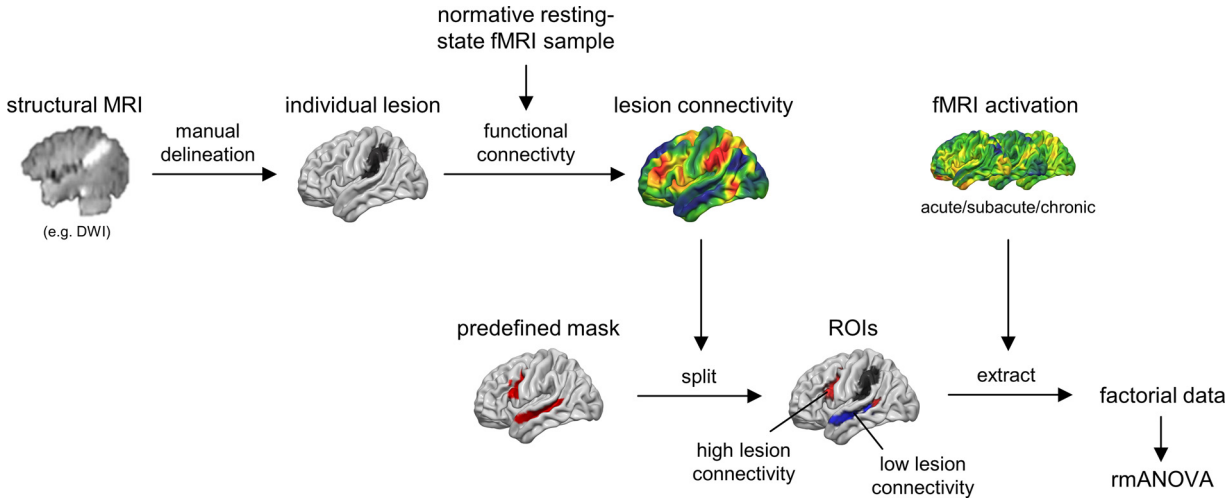

Fig. 1. Methodological overview.
See 'Material and methods' for explanations. Abbreviations: MRI = magnetic resonance imaging, DWI = diffusion weighted imaging, fMRI = functional MRI, ROIs = regions of interest, rmANOVA = repeated measurements analysis of variance.

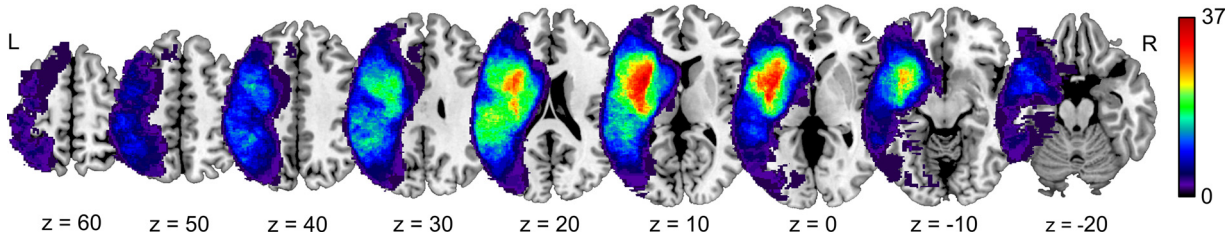

Fig. 2. Lesion overlay
Overlay of lesions of 71 patients with aphasia due to ischemic stroke with a maximum overlap of 37. Color indicates number of patients with a lesion in that voxel. Axial coordinates refer to MNI space.

1.83 s, echo time (TE): 25 ms, voxel size: 3 mm isotropic; Freiburg: 115 [paradigm II: 260] scans per session, TR: 2.19 s, TE: 30 ms, voxel size: 3 mm isotropic; Leipzig: 115 scans per session, TR: 1.89 s, TE: 25 ms, voxel size: 3 mm isotropic).

Additional MRI scans for anatomical reference and for lesion delineation included usual T1-weighted magnetization-prepared rapid acquisition with gradient echo (MPRAGE), T2-weighted fluid attenuated inversion recovery (FLAIR) as well as diffusion weighted EPI sequences.

3. Language testing

All patients were behaviorally characterized using the Aachen aphasia test (AAT, Huber et al., 1984) This multidimensional test includes formal rating of spontaneous speech (semi-standardized interview), comprehension (token test, auditory picture matching task, reading), repetition (phonemes, monosyllabic words, compound words, loan words, sentences), picture naming (simple objects, colors, compound words, situations) and written language (writing, combining words, reading).

Based on these subtests, we computed the language recovery score (LRS). This index score represents overall language performance at the different time points and allowed us to restrict the number of statistical tests to a reasonable amount. The LRS was defined as the sum of all AAT subscores divided by the maximum possible score. Behavioral scores were available from 54/55 acute, 67/69 subacute and 50/53 chronic measurements (see Fig. 3 and Supplementary Table 2).

Language recovery scores significantly improved from the acute to the subacute and from the subacute to the chronic measurement (paired t-tests, $n = 51/50$, both $p < 0.001$). The slope was significantly steeper from the acute to the subacute than from the subacute to the chronic measurement (paired t-test, $n = 41$, $p < 0.001$).

3.1. Normative sample

Resting-state fMRI scans obtained from 42 age and sex matched (age 59.4 ± 12.5; 54.8% male, all right handed) healthy participants (not to be confused with the healthy controls) were used to identify functional brain networks potentially affected by the patient's focal lesions in terms of a functional diaschisis effect. This data was obtained from the Enhanced Nathan Kline Institute Rockland Sample (http://fcon_1000.projects.nitrc.org/indi/enhanced/, Nooner et al., 2012). Scans were acquired on Siemens Trio 3 Tesla scanners. Resting-state fMRI was obtained using a multiband EPI sequence (TR 1.4 s, TE 30 ms, multiband factor: 4, voxel size: 2 mm isotropic, duration: 10 min). Structural T1-weighted images for anatomical reference were acquired with a MPRAGE sequence.

4. Data analysis

4.1. Lesion delineation

Lesions were manually delineated using MRIcron (ver. 2MAY2016, https://www.nitrc.org/projects/mricron) on the most appropriate available scan (typically acute DWI, subacute FLAIR or chronic T1-weighted scan). Fig. 2 provides the lesion overlay of all patients. Lesions of all except for two patients showed cortical involvement (see also SI Table 1).

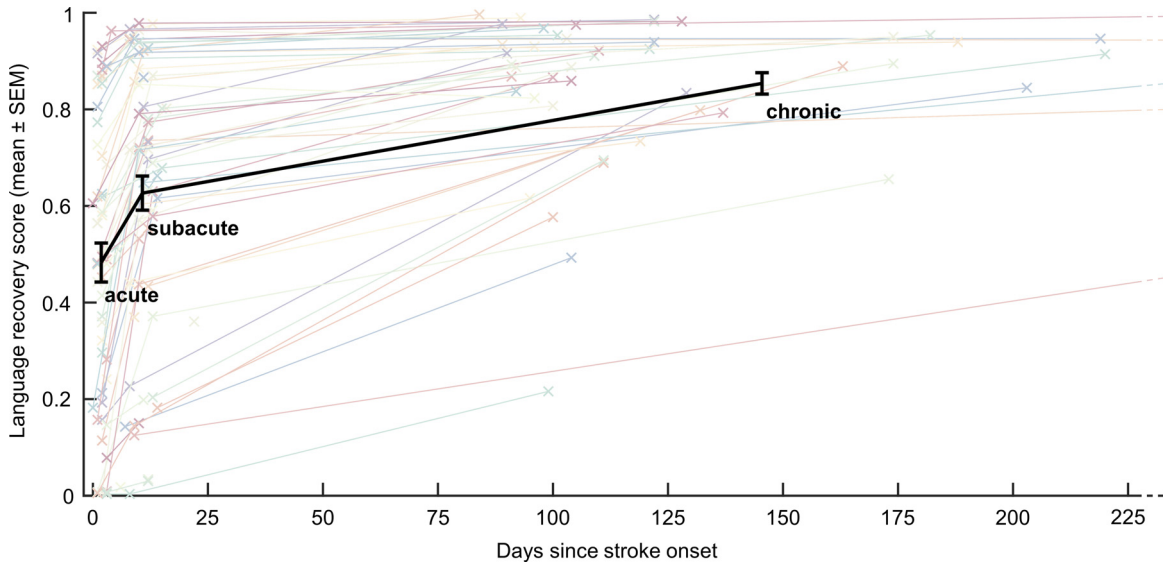

Fig. 3. Behavioral recovery
Behavioral recovery of all patients. Colored plots in the background represent all available individual language recovery scores (LRS). The black line represents the group mean. Error bars denote standard error of the mean (SEM). Note that the chronic measurement of five patients is beyond the range of the x-axis for display purposes.

Table 1
Repeated measures analysis of variance of fMRI activation and post-hoc tests.

Effect	F-value	p-value
Lesion connectivity	0.38	n.s.
Time	6.01	0.004
Time x Lesion connectivity	3.38	0.038

Effect	t-value	p-value
Time		
subacute > acute	3.6	< 0.001
chronic > acute	2.4	0.011
chronic > subacute	−0.9	n.s.
Time x Lesion connectivity		
subacute > acute x high > low	2.2	0.015
chronic > acute x high > low	1.5	n.s.
chronic > subacute x high > low	−1.3	n.s.

Longitudinal data from 44 patients was analyzed with regard to the factors time (acute, subacute, chronic) and lesion connectivity (high, low). We report results of F-Tests regarding both factors and their interaction. Post-hoc t-tests were performed for factors and interactions explaining a significant amount of variance. Bonferroni-correction was used to account for multiple comparisons. Reported p-values are uncorrected. Abbreviations: F/t-value = test statistic, p-value = probability value (one-tailed), n.s. = not significant.

4.2. Preprocessing

Analysis of fMRI data was performed with Statistical Parametric Mapping (SPM12, v7487, Wellcome Trust centre for Neuroimaging, London) and in-house tools with Matlab (2018b, MathWorks). We discarded the first four functional scans to allow for magnetic field saturation, applied slice time correction (sinc interpolation) and motion correction (two pass realignment using a least squares approach and a rigid body spatial transformation with six degrees of freedom). The structural T1-weighted image was coregistered (objective function: normalized mutual information) to the mean functional image and segmented using the unified segmentation approach (Ashburner and Friston, 2005). For patients, individual lesions were masked out prior to segmentation. Segmentation resulted in individual tissue probability maps and a nonlinear deformation field which was used to spatially normalize and resample all functional scans (4th degree B-spline interpolation to a voxel size of $3 \times 3 \times 3$ mm^3 for the event-related fMRI and $2 \times 2 \times 2$ mm^3 for the resting-state fMRI) and lesion masks ($1 \times 1 \times 1$ mm^3) to the MNI152 (Montreal Neurological Institute) space. To account for residual anatomical variance and to improve signal-to-noise ratio, all functional images were convolved with an isotropic Gaussian smoothing kernel with full width at half maximum of 8 mm for the event-related and 5 mm for the resting-state fMRI data.

4.3. Event-related fMRI

First level analysis was performed as a linear regression at each voxel (mass univariate approach), using generalized least squares with a global approximate AR(1) autocorrelation model and drift fit with Discrete Cosine Transform basis (128 s cut-off). Sentences with and without semantic violation of both conditions (Sp/Rev) were modelled separately as boxcar functions (defined by sentence onset and duration) convolved with the canonical hemodynamic response function as implemented in SPM12. The model additionally included the six motion parameters from the realignment as covariates of no interest. The **contrast** of interest was the differential activation Sp > Rev representing language specific activation. To account for global differences in fMRI activation magnitudes caused by the different MRI scanners and scanning parameters as well as the slightly different experimental paradigms, we performed a global **scaling** procedure. Uncorrected fMRI activation magnitudes showed considerable variability between sites/paradigms. We aimed to achieve comparable levels of activation across sites/paradigms. To this end, we determined a factor proportional to the magnitudes of fMRI activation in the group of healthy controls for each research site/paradigm separately. This factor was defined as the mean (per group/site) of the standard deviation (per control) across all voxels in the brain for the auditory main effect (i.e. Sp+Rev > rest). This factor was then multiplied with the number of sessions per control/patient. All contrast images (patients and healthy controls) were then divided by the corresponding factor.

Second level analysis (for the purpose of creating a global mask of regions potentially affected by diaschisis effects as described below) was carried out with random permutation testing (Nichols and Holmes, 2002). Inference was based on cluster size (p(FWE) < 0.05) given a cluster-forming threshold of $p < 0.005$ utilizing two-sample t-tests. The null-distribution of cluster sizes was approximated by 5000 random permutations of the group label.

4.4. Lesion network mapping

To identify brain networks potentially affected by the individual lesion, we used resting-state fMRI data from 42 healthy participants (Boes et al., 2015; Wawrzyniak et al., 2018). In addition to the preprocessing described for the task-based fMRI, we removed BOLD signal variance over time explained by the following nuisance variables using a multiple regression approach: motion parameters and their first derivative (as first and second order terms) and mean white matter and cerebrospinal fluid signal (as first order terms only). Residual BOLD time series were band-pass filtered with cut-off frequencies of 0.01 and 0.08 Hz. Finally, motion scrubbing was used to further improve data quality. This was achieved by calculation of framewise displacement (FD) defined as maximum frame to frame movement of any voxel within a 50 mm sphere centered in the sample volume (Power et al., 2012). All volumes with FD greater than 0.5 mm were discarded.

Regions of interest (ROIs) were defined as the gray matter portion of the individual brain lesions. This was achieved by removing all non-gray matter voxels from each patient's lesion based on individual tissue probability maps from the healthy participants (i.e. removing voxels with a gray matter probability of less than 50%). Representative BOLD time series for each ROI were then expressed as the first eigenvariate (Friston et al., 2006) of the time series of all remaining voxels (after excluding gray matter) within that ROI. Lesion networks were calculated in terms of **functional connectivity**, that is Fisher transformed (Fisher, 1915) Pearson correlation coefficients between ROI time series and the time series of all other voxels in the brain. Resulting connectivity maps were averaged across all resting-state fMRI datasets resulting in one (normative) functional connectivity map for each patient's individual lesion.

4.5. Statistic evaluation of diaschisis effects

Our hypothesis was that regions with high normative lesion connectivity might show a steeper increase in language specific activity over time than regions with low normative lesion connectivity. To test this hypothesis, we created a mask representing potential candidate regions for diaschisis effects defined by significantly less language specific activation (i.e. contrast Sp > Rev) in patients at any point in time (acute, $n = 55$; subacute, $n = 69$; chronic, $n = 53$) compared to the 14 healthy controls (conjunction null of two-sample t-tests, p(FWE) < 0.05 at the cluster-level, cluster forming threshold $p < 0.005$, see Fig. 1 and Fig. 5A). This mask was a priori restricted to regions with language specific activation in the healthy controls (i.e. the main effect of Sp > Rev in healthy controls). For every patient, the individual lesion (expanded by one voxel, i.e. 3 mm) was excluded from the mask. The mask was then divided into two regions for every patient: one region representing the quartile with the highest and another region representing the quartile with the lowest normative lesion connectivity (see Fig. 5B and 5C for spatial distribution of these regions on the group level). The remaining half of the mask was discarded. We then extracted mean individual fMRI effect sizes for language activation (i.e. Sp > Rev) within these regions. To focus on activation differences relative to controls, we subtracted the mean language activation of healthy controls from patient's language activation. Finally, a 3 × 2 factorial rmANOVA ($n = 44$ complete longitudinal data sets) with the factors time (acute, subacute, and chronic) and lesion connectivity (high, low) as well as their interaction was performed using IBM SPSS Statistics (version 24.0.0.0). See SI Table 3 for mean and standard deviation of all six cells of this rmANOVA. Degrees of freedom were adjusted according to Greenhouse-Geisser whenever the assumption of sphericity was violated as indicated by the Mauchly-test ($p < 0.05$). Post-hoc paired t-tests (Bonferroni corrected) were applied to the same data conditional on significant F-tests. For the main effect of time this means that we tested subacute > acute, chronic > acute and chronic > subacute activation (regardless of lesion connectivity) in a paired *t*-test. For the interaction 'time x lesion connectivity', we performed the same tests using the difference of activity in regions with high and low (i.e. high - low) lesion connectivity. With this contrast (high - low), diaschisis effects would be signed negative and resolution of diaschisis would be signed positive. One-tailed tests were performed based on our hypotheses, because we wanted to specifically test for increasing fMRI activity over time. Contrasting activity in regions with high and low connectivity controls for confounding effects (underactivation caused by hypoperfusion, disturbed neurovascular coupling or poor behavioral performance).

To test for differences in the **spatial distribution** of the regions with high and low lesion connectivity, we performed a random permutation test (Nichols and Holmes, 2002) with regard to the absolute difference of the occurrence of labels 'high' and 'low' per voxel. To assess the null-distribution of this difference, we randomly assigned the labels 'high' and 'low' for each patient and computed the maximum difference across all voxels within the predefined mask 5000 times. The real difference (with correctly assigned labels) was then thresholded at p(FWE) < 0.05 on the voxel-level (corresponding to an absolute difference > 21 for both tails).

4.6. Correlation analysis

To test for behavioral relevance of diaschisis effects, we performed linear (i.e., Pearson) correlation analysis between diaschisis effect sizes (high > low) and global language performance (i.e. LRS) for all available patients. Additionally, we tested for correlations between longitudinal changes of fMRI activation and changes of language recovery scores.

4.7. Data and code availability

Unfortunately, the datasets analyzed in the current study may not be made publicly available due to the data protection agreement (approved by the local ethics committees) signed by the participants. Data can be shared upon request based on a formal data sharing agreement. All used software packages are referenced in the methods section.

5. Results

5.1. Diaschisis effects

We analyzed fMRI language activation (i.e. Sp > Rev) with respect to normative functional connectivity to the individual lesion site, because diaschisis effects per definition must depend on connectivity to the lesion.

Language activation in regions with high and low connectivity to the individual stroke lesion was extracted at all three points in time (acute, subacute and chronic) separately (see Fig. 4A and Supplementary Table 3). To highlight deviations from normal activation patterns, mean language activation from healthy controls was subtracted from patient's activation. This means, that the dashed baselines at zero in Fig. 4 correspond to normal levels of language activation as seen in healthy controls while values below that line correspond to underactivation in patients compared to controls. Looking at Fig. 4A, we saw activation mostly below the level of controls in both conditions at all points in time. Additionally, activation was significantly lower in regions with high than low normative connectivity to the lesion at the acute time point (paired *t*-test, $T = 2.3$, $p = 0.01$) corresponding to a possible diaschisis effect.

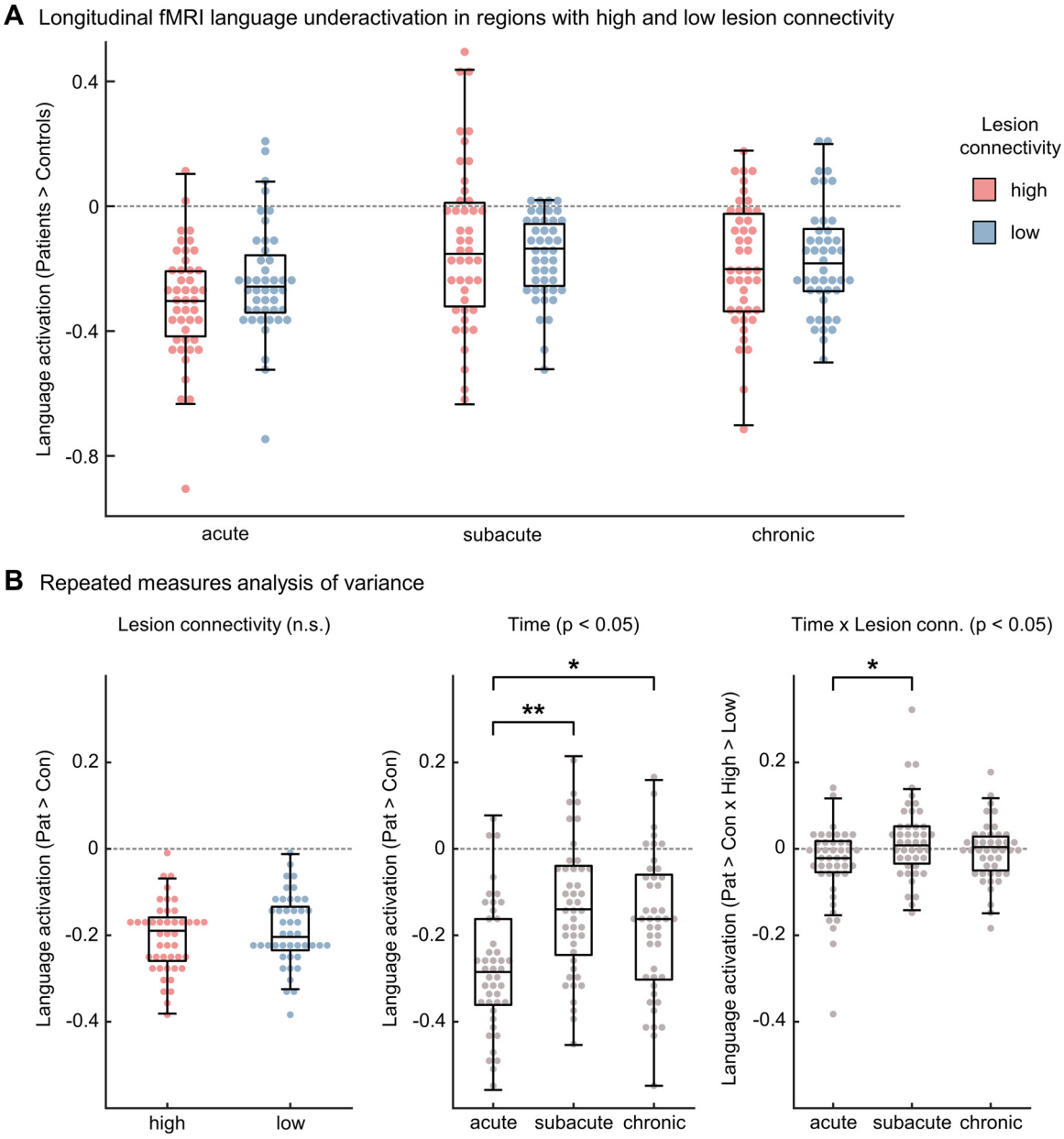

Fig. 4. Functional magnetic resonance imaging activation of 44 patients with aphasia.
Panel A displays longitudinal (acute, subacute, chronic) fMRI language activation (speech > reversed speech) in regions with high (red) and low (blue) lesion connectivity. Effect sizes of healthy controls have been subtracted to specifically examine stroke induced effects. The dashed line at zero therefore represents normal activity levels as observed in healthy controls while values below that line indicate underactivation. Panel B visualizes the rmANOVA results and shows both factors and their interaction. Results from F-tests are shown in parenthesis (n.s. = not significant). Significant differences after Bonferroni correction in the post-hoc t-tests are indicated by stars ($p < 0.05$, **$p < 0.001$, one-tailed). In both panels, all presented values are mean scaled beta estimates extracted from the fMRI first level analysis (arbitrary units). For display purposes, all data was residualized for the subject factor to account for the within-subject design. Central marks of the box represent the median value, the edges are the 25th and 75th percentiles, and the whiskers extend to the most extreme data points not more than 150% of the interquartile range beyond the boxes. Filled circles represent individual data points.*

In line with our hypothesis, underactivation seemed to be most pronounced at the acute time point in regions with high normative connectivity and to return to normal over time, compatible with the phenomenon of resolution of diaschisis. To statistically test our hypothesis, we performed a 2 × 3 repeated measures ANOVA with the factors lesion connectivity (high, low) and time (acute, subacute, chronic) based on 44 complete longitudinal data sets. Both factors and the interaction 'time x lesion connectivity' satisfied the assumption of sphericity according to the Mauchly-test ($p > 0.05$). Post-hoc Bonferroni-corrected t-tests were performed when a factor or interaction explained a significant fraction of variance. The results are displayed in Fig. 4B and Table 1.

We found that the factor 'time' explained a significant amount of variance (Fig. 4B, middle panel). Bonferroni corrected post-hoc t-tests showed a significant increase in language activation from the acute to the subacute and from the acute to the chronic measurement. This increase might be partially caused by reperfusion of the ischemic penumbra. Our main research question, however, was whether increase in activation depends on connectivity to the lesion. Although there was no effect of lesion connectivity per se (Fig. 4B left panel), the interaction 'time x lesion connectivity' explained a significant amount of variance (Fig. 4B right panel). This demonstrates that temporal dynamics in language specific activation indeed depend on lesion connectivity. Bon-

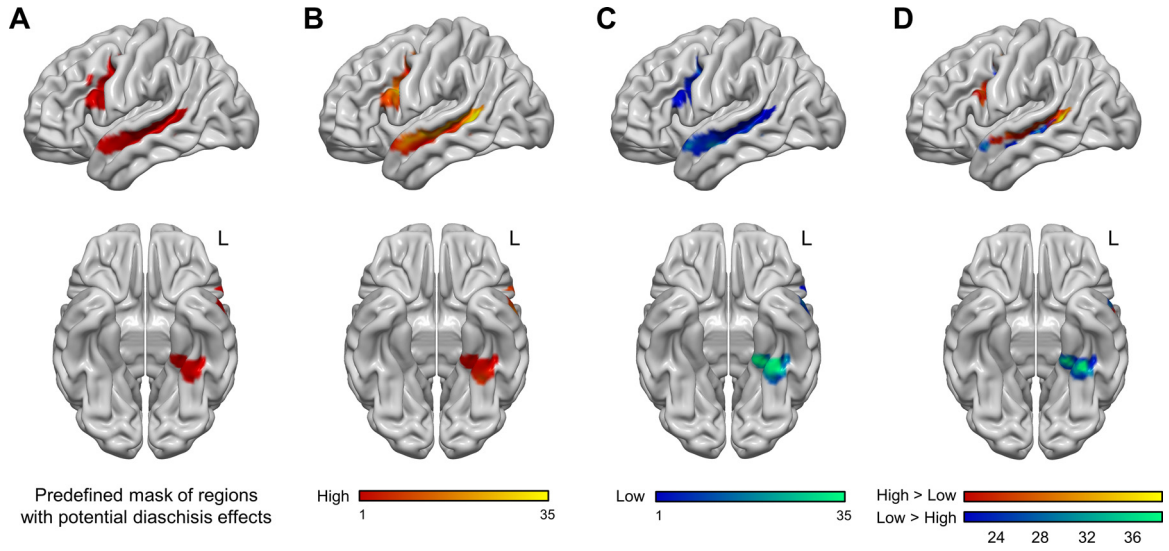

Fig. 5. Predefined mask and spatial distribution of regions with high and low lesion connectivity.
Panel A displays the predefined mask (red) of candidate regions affected by potential diaschisis effects on the group level defined by significantly less activation of patients at any point in time compared to healthy controls (conjunction null of two-sample t-tests, p(FWE) < 0.05 at the cluster-level, cluster forming threshold $p < 0.005$). Panel B and C show the spatial distribution (overlap) of regions with high and low lesion connectivity in all 71 patients. Panel D shows differences in this distribution between regions with high and low lesion connectivity (random permutation test with 5000 permutations, p(FWE) < 0.05 on the voxel-level). The contrast high > low is shown in warm and the opposite contrast in cool colors. Numbers refer to absolute difference in occurrence of the labels high and low lesion connectivity. The upper row shows lateral surface renderings of the left hemisphere; the lower row shows renderings of the inferior brain surface. Abbreviations: L: left.

ferroni corrected post-hoc t-tests demonstrated a significantly steeper increase in language specific fMRI activation in regions with high than in regions with low lesion connectivity from the acute to the subacute phase. This could be explained by a distinct diaschisis effect in regions with high lesion connectivity in the acute phase, which (at least partially) resolves from the acute to the subacute phase. Of note, the subtraction of language activation of healthy controls (measured once) from language activation of patients (measured longitudinally) does not influence the results of all statistical tests performed longitudinally.

We were also interested in the **spatial distribution** of the regions with high and low lesion connectivity in all 71 patients (Fig. 5B and 5C) within the predefined mask (Fig. 5A) and indeed found specific differences (Fig. 5D). Regions with high lesion connectivity (where we would expect diaschisis effects) were located significantly more frequently in left frontotemporal cortical areas, especially in the inferior frontal gyrus (pars triangularis and opercularis), and the middle temporal gyrus, especially in the posterior portion. Regions with low lesion connectivity were more frequently found in the left inferior temporal and fusiform gyri.

5.2. Correlation with behavioral data

To test for behavioral relevance of the described effects on fMRI activation, we performed correlation analyses between differential fMRI effect sizes and global severity of aphasia. Since we were particularly interested in the interaction 'time x lesion connectivity', we performed linear (i.e. Pearson) correlation analyses between the effect of 'lesion connectivity' (difference of mean fMRI activation in regions with high and low – i.e. high minus low – connectivity to the lesion) with the language recovery score (LRS) for each point in time separately (see first three columns of Table 2).

We found a significant correlation between LRS and lesion connectivity-dependent language activation at the subacute measurement ($n = 67$, $p = 0.003$, significant after Bonferroni correction, see Fig. 6A). Better language performance (in terms of LRS values) was associated with higher language activation in regions with high compared to low lesion connectivity. We argue that low values in this contrast reflect a diaschisis effect because they denote less language activation in regions with high lesion connectivity compared to regions with low lesion connectivity. Therefore, the described positive correlation indicates that less diaschisis (or more resolution of diaschisis) at the subacute measurement is related to better language performance.

As our conclusions are mainly based on longitudinal changes in fMRI activation, we additionally performed correlation analyses between longitudinal changes of fMRI effect sizes and LRS (see last three columns of Table 2). Here, we found a significant association between resolution of the language specific diaschisis effect (i.e. Δ high > low) and behavioral improvement (Δ LRS) from the subacute to the chronic measurement ($n = 50$, $p = 0.003$, significant after Bonferroni correction, see Fig. 6B).

6. Discussion

This is the first study examining functional diaschisis effects and their functional relevance in patients with acute aphasia due to ischemic stroke by combining lesion network mapping with longitudinal task-based fMRI. Our hypothesis was that resolution of lesion-distant neural dysfunction (diaschisis), operationalized by increasing language specific fMRI activation, would be located predominantly in regions with high normative connectivity to the lesion site as assessed with resting-state fMRI data from healthy participants. In accordance with our hypothesis, we found a significantly steeper increase of language specific activation from the acute to the subacute measurement in regions with high than in regions with low lesion connectivity. We interpret this increase in activation as resolution of the diaschisis effect in functional networks affected by the lesion. The behavioral relevance of this effect is shown by a significant correlation between global language scores and the size of the diaschisis effect at the subacute measurement. Specifically, higher language specific activation in regions with high compared to low lesion connectivity was associated with better global language performance. The link between diaschisis and the language deficit in the early phase post stroke is particularly plausible given the spatial distribution of regions with high compared to those with low lesion connectivity (Fig. 5D) which closely resembled core language regions in the inferior frontal gyrus and the middle temporal gyrus mostly pronounced in its posterior

Table 2
Correlation between diaschisis effects and aphasia severity.

	acute	subacute	chronic	acute-subacute	subacute-chronic	acute-chronic
r =	−0.11	0.36*	−0.07	−0.20	0.41*	−0.08
p =	0.44	0.003	0.60	0.15	0.003	0.63
n =	54	67	50	51	50	41

Pearson correlation analyses between lesion connectivity specific language activation (i.e. high > low) and language recovery score were calculated for each measurement (acute, subacute, chronic) and for longitudinal changes between the measurements (acute-subacute, subacute-chronic, acute-chronic) using all available data. Positive r-values indicate that higher language activation in regions with high compared to low lesion connectivity (i.e. less diaschisis) correlates with better language performance or that resolution of diaschisis correlates with behavioral improvement, respectively. Reported p-values are uncorrected. Asterisks indicate significant correlations after Bonferroni correction. Abbreviations: r = correlation coefficient, p = probability value, n = number of data points (i.e. patients).

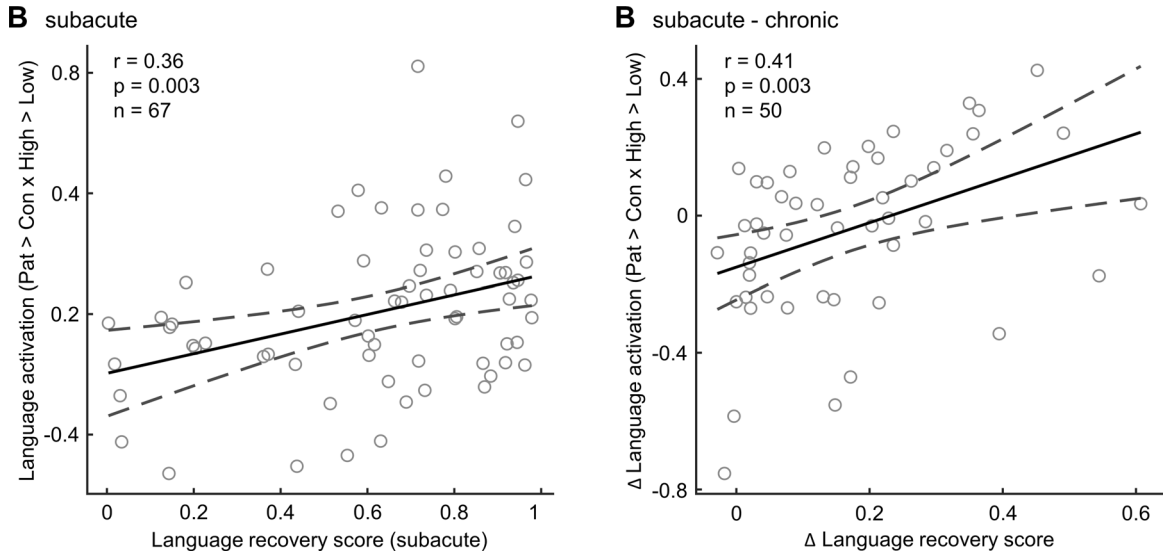

Fig. 6. Correlation between diaschisis effect and language performance.
*(A) In the subacute measurement, there was a significant correlation between a language specific diaschisis effect (*i.e. *high > low lesion connectivity) and language recovery score. The positive association means that less diaschisis correlates with better language performance. (B) Improvements in these two measures from the subacute to the chronic phase were also significantly correlated. Solid lines represent best linear fit with its 95% confidence interval (dashed lines). Circles are individual data points. Abbreviations: r = correlation coefficient, p = probability value, n = number of data points (*i.e. *patients), Pat = Patients, Con = Controls.*

portion (Binder et al., 2009; Noonan et al., 2013; Rodd et al., 2015). Our data suggest that language deficits in the early phase after stroke are partially caused by functional diaschisis effects in frontotemporal core areas for language processing. This means that regions previously functionally connected to the lesion site become dysfunctional because of the missing input from the lesion site. In turn, this leads to less language specific activation in these regions.

Importantly, while previous studies on diaschisis in aphasic patients focused solely on subcortical lesions (Boes et al., 2015; Hillis et al., 2002; Vallar et al., 1988; Weiller et al., 1993), we here provide evidence for diaschisis in functional networks mostly affected by cortical infarcts. Furthermore, improvement of aphasia might be partially caused by resolution of functional diaschisis. Indeed, the corresponding correlation analysis of longitudinal behavioral changes and longitudinal changes in differential fMRI activation demonstrated a significant association of behavioral recovery and resolution of the functional diaschisis effect, which, however, was found from the subacute to the chronic phase. Nevertheless, our behavioral data (Fig. 3) confirmed the previously described pattern of highly dynamic language recovery in the early phase which then decelerates over time (Pedersen et al., 1995). We therefore interpret our data in the sense that the early behavioral improvement seen in many aphasic patients might be caused by resolution of diaschisis to a significant degree. This is in line with previous studies that show that resolution of diaschisis occurs mainly within the first days to weeks after stroke onset (Carrera and Tononi, 2014; Witte et al., 2000).

In the study of diaschisis, the added value of combining task-based fMRI and lesion network mapping is of particular importance. In previous studies, task-based fMRI in acute aphasic stroke patients showed an acute decrease in language specific activation in both hemispheres which then resolved over time as a possible correlate of diaschisis (Saur et al., 2006; Stockert et al., 2020). Using this method in isolation, however, it remained unclear whether the longitudinal dynamics in activation (or which part of it) depends on connectivity to the lesion as one would expect in diaschisis. On the other hand, studies solely using lesion network mapping demonstrated a relationship between normative lesion connectivity to Broca's area and aphasia in patients with subcortical lesions (Boes et al., 2015). Yet, in this study it remained unclear whether a dysfunction in Broca's area indeed caused the aphasia. Alternatively, involvement of the lesioned subcortical areas (all functionally connected to Broca's area) in language processing could have led to aphasia. The combination of both methods, as implemented in our study, allows demonstrating an acute decrease in activation which then partially resolves over time. This resolution is significantly more pronounced in regions with functional connections to the lesion. In our opinion, this operationalization of the diaschisis effect and its resolution is the closest one described in the literature so far.

Alternative mechanisms contributing to early post-stroke fMRI activation changes include hypo- and reperfusion of the ischemic penumbra (Hillis et al., 2008; Hossmann, 1994). The current analysis used existing data from research projects that primarily aimed at characterizing language recovery after aphasic stroke with no specific focus on diaschisis. Therefore, no perfusion measurements were performed. We argue, that effects of reperfusion are represented by the main effect of 'time' with an increase of language activity mainly from the acute to the subacute time point while the interaction 'time x lesion connectivity' specifically demonstrates an additional lesion connectivity dependent increase in language activity representing resolution of diaschisis. This is based on the assumption that the dependency of dynamics in fMRI activation on normative lesion connectivity (represented by the interaction 'time x lesion connectivity') cannot be explained by vascular effects because functional networks are independent of vascular territories (Beckmann et al., 2005). It should be noted though, that regions with high lesion connectivity tended to belong to the territory of the middle cerebral artery while regions with low lesion connectivity more frequently belonged to the vertebrobasilar territory (see Fig. 5D). To address this limitation, we repeated the original analysis with a small modification. We used distance maps instead of lesion network maps to define regions near to the lesion (i.e. in the ischemic penumbra) and remote from the lesion (i.e. outside the ischemic penumbra). Each distance map encodes the (shortest) distance to the individual stroke lesion (see Supplementary Information for methodological details). We would expect reperfusion effects mainly in regions near to the lesion and not or to a lesser extent in regions remote from the lesion. The overall results were comparable to the original analysis (cf. Table 1). However, the interaction 'time x proximity' did not reach significance. Therefore, subacute reactivation was the same in regions near to the lesion (i.e. ischemic penumbra) and remote from the lesion. Additionally, none of the correlation analyses (analogous to Table 2) was significant. In sum, this additional analysis could not support the hypothesis, that reperfusion of the ischemic penumbra was driving subacute reactivation. Similarly, less fMRI activation in acute stroke patients could also be caused by a failure of the BOLD signal due to an acute disruption of the neurovascular coupling (Krainik et al., 2005). However, by contrasting language activation in regions with high and low lesion connectivity, we again minimize the potential impact of such effects because it can be assumed that BOLD-failure would affect the whole vascular territory and not only regions functionally connected to the lesion. In addition, longitudinal BOLD signal changes in stroke patients have been shown to reflect changes in neural activity rather than resolution of disrupted neurovascular coupling (Geranmayeh et al., 2015). The same applies to in-scanner performance. One might argue that acute fMRI underactivation could be caused by less engagement in the task as in-scanner performance is decreased mostly at the acute measurement (see Supplementary Table 2). While the main effect of 'time' could be interpreted in such a way, our main finding of a 'time x connectivity' interaction is not impressible by this argument because a performance associated decrease of activation would not dependent on lesion connectivity.

Finally, we would like to address some limitations of our study. First, our interpretation that resolution of diaschisis leads to behavioral improvement is fundamentally linked to the correlation analysis of longitudinal *changes* in fMRI activation and behavioral scores. In contrast to our hypothesis, there was no such longitudinal correlation of behavioral improvement and the resolution of diaschisis from the acute to the subacute phase. On the one hand, the absence of this correlation in our data might be caused by confounding reperfusion effects. As mentioned before, hypoperfusion and reperfusion have an impact on acute behavioral performance and therefore partially mask effects driven by diaschisis and its resolution. Indeed, we found a significant correlation of mean fMRI activation (regardless of lesion connectivity) and behavioral performance in the acute phase ($r = 0.28$, $p = 0.04$, $n = 54$) in an exploratory analysis. Although we have argued in favor of the validity of differential fMRI effect sizes also in the acute phase, these arguments do not apply to the behavioral data. This might explain the fact that our data supports acute resolution of diaschisis in terms of connectivity specific fMRI reactivation but without correlating with behavioral improvement. On the other hand, we found a significant correlation in the time period between the subacute and chronic measurement. Diaschisis is expected to resolve mainly within the first days to weeks after stroke (Carrera and Tononi, 2014). Nevertheless, the time period from the subacute (Ø = day 11) to the chronic (Ø = day 150) measurement partially overlaps with the early post-stroke phase (~ first few weeks). Therefore, we speculate that the described longitudinal correlation from the subacute to the chronic measurement might nevertheless reflect behavioral improvement caused by resolution of diaschisis in the first few weeks. Alternatively, diaschisis effects might partially persist substantially longer than a few weeks after stroke onset (DeMarco and Turkeltaub, 2020; Price et al., 2001) and therefore might render it a potential target for adjuvant non-invasive brain stimulation in neurorehabilitation. Second, the present study exclusively considers damage to gray matter. Future efforts might additionally incorporate structural connectome data to identify fiber tracts and corresponding cortical regions affected by disconnection mechanisms due to white matter damage (Foulon et al., 2018; Fox, 2018; Yourganov et al., 2016). Third, in lesion network mapping, lesions are used as regions of interest for resting-state functional connectivity analyses. However, these regions of interest follow vascular territories and might thus be very heterogeneous in terms of functional anatomy. They range from small lesions in a single functional network to large lesions spanning multiple functional networks. This might lead to some bias in the corresponding lesion network maps which might be less accurate and less meaningful with increasing lesion sizes (Boes, 2021). Finally, we exclusively studied post-stroke aphasia. Yet, our methodological approach might also be of value for other stroke induced (higher order) deficits or even data sets featuring multiple behavioral domains.

7. Conclusion

We combined lesion network mapping and task-based fMRI to examine resolution of functional diaschisis effects in patients with post-stroke aphasia due to cortical infarctions. We found that resolution of neural dysfunction, as expressed by an increase of fMRI activation over time distant to the lesion, depends on normative functional connectivity to the lesion site. Because this effect was behaviorally relevant, we argue that resolution of diaschisis might be a relevant mechanism contributing to the early fast behavioral improvement often seen in patients with aphasia. Additionally, the presented data demonstrate that lesion network mapping is a suitable approach to study diaschisis effects based solely on the lesion location inferred from clinical imaging.

Funding

This work was supported by intramural funds. Dorothee Saur and Julian Klingbeil (SA 1723/5-1) and Gesa Hartwigsen (HA 6314/3-1 and HA 6314/4-1) were supported by the Deutsche Forschungsgemeinschaft. Dorothee Saur was funded by the James S. McDonnell Foundation by a scholar award (Understanding Human Cognition, #220020292). Max Wawrzyniak was supported by the Clinician Scientist Program of the Medical Faculty of the University of Leipzig. Open Access Publishing was supported by Leipzig University.

Author contributions

Conceptualization, MW, DS; Investigation, MW, JK, AS, DS; Software, MW; Methodology, MW; Formal Analysis, MW, HS; Writing – Original Draft, MW; Writing – Review & Editing, MW, HS, JK, AS, GH, CW, DS

Data and code availability

Unfortunately, the datasets analyzed in the current study may not be made publicly available due to the data protection agreement (approved by the local ethics committees) signed by the participants. Data can be shared upon request based on a formal data sharing agreement. All used software packages are referenced in the methods section.

Supplementary materials

Supplementary material associated with this article can be found, in the online version, at doi:10.1016/j.neuroimage.2022.119001.

References

Ashburner, J., Friston, K.J., 2005. Unified segmentation. Neuroimage 26, 839–851. doi:10.1016/j.neuroimage.2005.02.018.

Beckmann, C.F., DeLuca, M., Devlin, J.T., Smith, S.M., 2005. Investigations into resting-state connectivity using independent component analysis. Philos. Trans. R. Soc. Lond., B, Biol. Sci. 360, 1001–1013. doi:10.1098/rstb.2005.1634.

Binder, J.R., Desai, R.H., Graves, W.W., Conant, L.L., 2009. Where is the semantic system? A critical review and meta-analysis of 120 functional neuroimaging studies. Cerebral cortex (New York, N.Y.: 1991) 19, 2767–2796. doi:10.1093/cercor/bhp055.

Boes, A.D., 2021. Lesion network mapping: where do we go from here? Brain 144, e5. doi:10.1093/brain/awaa350.

Boes, A.D., Prasad, S., Liu, H., Liu, Q., Pascual-Leone, A., Caviness, V.S., Fox, M.D., 2015. Network localization of neurological symptoms from focal brain lesions. Brain 138, 3061–3075. doi:10.1093/brain/awv228.

Brownsett, S.L.E., Warren, J.E., Geranmayeh, F., Woodhead, Z., Leech, R., Wise, R.J.S., 2014. Cognitive control and its impact on recovery from aphasic stroke. Brain 137, 242–254. doi:10.1093/brain/awt289.

Cappa, S.F., Perani, D., Grassi, F., Bressi, S., Alberoni, M., Franceschi, M., Bettinardi, V., Todde, S., Fazio, F., 1997. A PET follow-up study of recovery after stroke in acute aphasics. Brain Lang 56, 55–67.

Carrera, E., Tononi, G., 2014. Diaschisis: past, present, future. Brain 137, 2408–2422. doi:10.1093/brain/awu101.

Corbetta, M., Kincade, M.J., Lewis, C., Snyder, A.Z., Sapir, A., 2005. Neural basis and recovery of spatial attention deficits in spatial neglect. Nat. Neurosci. 8, 1603–1610. doi:10.1038/nn1574.

DeMarco, A.T., Turkeltaub, P.E., 2020. Functional anomaly mapping reveals local and distant dysfunction caused by brain lesions. Neuroimage 215, 116806. doi:10.1016/j.neuroimage.2020.116806.

Engelter, S.T., Gostynski, M., Papa, S., Frei, M., Born, C., Ajdacic-Gross, V., Gutzwiller, F., Lyrer, P.A., 2006. Epidemiology of aphasia attributable to first ischemic stroke: incidence, severity, fluency, etiology, and thrombolysis. Stroke 37, 1379–1384. doi:10.1161/01.STR.0000221815.64093.8c.

Fisher, R.A., 1915. Frequency distribution of the values of the correlation coefficient in samples from an indefinitely large population. Biometrika 10, 507. doi:10.2307/2331838.

Foulon, C., Cerliani, L., Kinkingnéhun, S., Levy, R., Rosso, C., Urbanski, M., Volle, E., Thiebaut de Schotten, M., 2018. Advanced lesion symptom mapping analyses and implementation as BCBtoolkit. Gigascience 7, 1–17. doi:10.1093/gigascience/giy004.

Fox, M.D., 2018. Mapping symptoms to brain networks with the human connectome. New Eng J Med 379, 2237–2245. doi:10.1056/NEJMra1706158.

Friston, K.J., Rotshtein, P., Geng, J.J., Sterzer, P., Henson, R.N., 2006. A critique of functional localisers. Neuroimage 30, 1077–1087. doi:10.1016/j.neuroimage.2005.08.012.

Geranmayeh, F., Brownsett, S.L.E., Wise, R.J.S., 2014. Task-induced brain activity in aphasic stroke patients: what is driving recovery? Brain 137, 2632–2648. doi:10.1093/brain/awu163.

Geranmayeh, F., Wise, R.J.S., Leech, R., Murphy, K., 2015. Measuring vascular reactivity with breath-holds after stroke: a method to aid interpretation of group-level BOLD signal changes in longitudinal fMRI studies. Hum Brain Mapp 36, 1755–1771. doi:10.1002/hbm.22735.

Grefkes, C., Nowak, D.A., Eickhoff, S.B., Dafotakis, M., Küst, J., Karbe, H., Fink, G.R., 2008. Cortical connectivity after subcortical stroke assessed with functional magnetic resonance imaging. Ann. Neurol. 63, 236–246. doi:10.1002/ana.21228.

He, B.J., Snyder, A.Z., Vincent, J.L., Epstein, A., Shulman, G.L., Corbetta, M., 2007. Breakdown of functional connectivity in frontoparietal networks underlies behavioral deficits in spatial neglect. Neuron 53, 905–918. doi:10.1016/j.neuron.2007.02.013.

Hillis, A.E., Gold, L., Kannan, V., Cloutman, L., Kleinman, J.T., Newhart, M., Heidler-Gary, J., Davis, C., Aldrich, E., Llinas, R., Gottesman, R.F., 2008. Site of the ischemic penumbra as a predictor of potential for recovery of functions. Neurology 71, 184–189. doi:10.1212/01.wnl.0000317091.17339.98.

Hillis, A.E., Heidler, J., 2002. Mechanisms of early aphasia recovery. Aphasiology 16, 885–895. doi:10.1080/0268703.

Hillis, A.E., Wityk, R.J., Barker, P.B., Beauchamp, N.J., Gailloud, P., Murphy, K., Cooper, O., Metter, E.J., 2002. Subcortical aphasia and neglect in acute stroke: the role of cortical hypoperfusion. Brain 125, 1094–1104. doi:10.1093/brain/awf113.

Holland, A., Fromm, D., Forbes, M., MacWhinney, B., 2017. Long-term Recovery in Stroke Accompanied by Aphasia: a Reconsideration. Aphasiology 31, 152–165. doi:10.1080/02687038.2016.1184221.

Hope, T.M.H., Leff, A.P., Prejawa, S., Bruce, R., Haigh, Z., Lim, L., Ramsden, S., Oberhuber, M., Ludersdorfer, P., Crinion, J., Seghier, M.L., Price, C.J., 2017. Right hemisphere structural adaptation and changing language skills years after left hemisphere stroke. Brain 140, 1718–1728. doi:10.1093/brain/awx086.

Hossmann, K.A., 1994. Viability thresholds and the penumbra of focal ischemia. Ann. Neurol. 36, 557–565. doi:10.1002/ana.410360404.

Huber, W., Poeck, K., Willmes, K., 1984. The Aachen aphasia test. Adv Neurol 42, 291–303.

Kim, Y.W., Kim, H.S., An, .Y..-S., 2012. Statistical mapping analysis of brain metabolism in patients with subcortical aphasia after intracerebral hemorrhage: a pilot study of F-18 FDG PET images. Yonsei Med. J. 53, 43–52. doi:10.3349/ymj.2012.53.1.43.

Klingbeil, J., Wawrzyniak, M., Stockert, A., Karnath, H.-O., Saur, D., 2020. Hippocampal diaschisis contributes to anosognosia for hemiplegia: evidence from lesion network-symptom-mapping. Neuroimage 208, 116485. doi:10.1016/j.neuroimage.2019.116485.

Krainik, A., Hund-Georgiadis, M., Zysset, S., Cramon, D.Y.von, 2005. Regional impairment of cerebrovascular reactivity and BOLD signal in adults after stroke. Stroke 36, 1146–1152. doi:10.1161/01.STR.0000166178.40973.a7.

Laska, A.C., Hellblom, A., Murray, V., Kahan, T., Arbin, M.von, 2001. Aphasia in acute stroke and relation to outcome. J. Intern. Med. 249, 413–422.

Laska, A.C., Kahan, T., Hellblom, A., Murray, V., Arbin, M.von, 2011. A randomized controlled trial on very early speech and language therapy in acute stroke patients with aphasia. Cerebrovasc Dis Extra 1, 66–74. doi:10.1159/000329835.

Lazar, R.M., Speizer, A.E., Festa, J.R., Krakauer, J.W., Marshall, R.S., 2008. Variability in language recovery after first-time stroke. J. Neurol. Neurosurg. Psychiatr. 79, 530–534. doi:10.1136/jnnp.2007.122457.

Nadeau, S.E., Crosson, B., 1997. Subcortical aphasia. Brain Lang 58, 355–402. doi:10.1006/brln.1997.1707, discussion 418-23.

Nichols, T.E., Holmes, A.P., 2002. Nonparametric permutation tests for functional neuroimaging: a primer with examples. Hum Brain Mapp 15, 1–25.

Noonan, K.A., Jefferies, E., Visser, M., Lambon Ralph, M.A., 2013. Going beyond inferior prefrontal involvement in semantic control: evidence for the additional contribution of dorsal angular gyrus and posterior middle temporal cortex. J Cogn Neurosci 25, 1824–1850. doi:10.1162/jocn_a_00442.

Nooner, K.B., Colcombe, S.J., Tobe, R.H., Mennes, M., Benedict, M.M., Moreno, A.L., Panek, L.J., Brown, S., Zavitz, S.T., Li, Q., Sikka, S., Gutman, D., Bangaru, S., Schlachter, R.T., Kamiel, S.M., Anwar, A.R., Hinz, C.M., Kaplan, M.S., Rachlin, A.B., Adelsberg, S., Cheung, B., Khanuja, R., Yan, C., Craddock, C.C., Calhoun, V., Courtney, W., King, M., Wood, D., Cox, C.L., Kelly, A.M.C., Di Martino, A., Petkova, E., Reiss, P.T., Duan, N., Thomsen, D., Biswal, B., Coffey, B., Hoptman, M.J., Javitt, D.C., Pomara, N., Sidtis, J.J., Koplewicz, H.S., Castellanos, F.X., Leventhal, B.L., Milham, M.P., 2012. The NKI-rockland sample: a model for accelerating the pace of discovery science in psychiatry. Front Neurosci 6, 152. doi:10.3389/fnins.2012.00152.

Pedersen, P.M., Jørgensen, H.S., Nakayama, H., Raaschou, H.O., Olsen, T.S., 1995. Aphasia in acute stroke: incidence, determinants, and recovery. Ann. Neurol. 38, 659–666. doi:10.1002/ana.410380416.

Perani, D., Vallar, G., Cappa, S., Messa, C., Fazio, F., 1987. Aphasia and neglect after subcortical stroke. A clinical/cerebral perfusion correlation study. Brain 110 (Pt 5), 1211–1229. doi:10.1093/brain/110.5.1211.

Power, J.D., Barnes, K.A., Snyder, A.Z., Schlaggar, B.L., Petersen, S.E., 2012. Spurious but systematic correlations in functional connectivity MRI networks arise from subject motion. Neuroimage 59, 2142–2154. doi:10.1016/j.neuroimage.2011.10.018.

Price, C.J., Warburton, E.A., Moore, C.J., Frackowiak, R.S., Friston, K.J., 2001. Dynamic diaschisis: anatomically remote and context-sensitive human brain lesions. J Cogn Neurosci 13, 419–429.

Rodd, J.M., Vitello, S., Woollams, A.M., Adank, P., 2015. Localising semantic and syntactic processing in spoken and written language comprehension: an Activation Likelihood Estimation meta-analysis. Brain Lang 141, 89–102. doi:10.1016/j.bandl.2014.11.012.

Saur, D., Kreher, B.W., Schnell, S., Kümmerer, D., Kellmeyer, P., Vry, M.-.S., Umarova, R., Musso, M., Glauche, V., Abel, S., Huber, W., Rijntjes, M., Hennig, J., Weiller, C., 2008. Ventral and dorsal pathways for language. In: Proceedings of the National Academy of Sciences of the United States of America 105, pp. 18035–18040. doi:10.1073/pnas.0805234105.

Saur, D., Lange, R., Baumgaertner, A., Schraknepper, V., Willmes, K., Rijntjes, M., Weiller, C., 2006. Dynamics of language reorganization after stroke. Brain 129, 1371–1384. doi:10.1093/brain/awl090.

Saur, D., Ronneberger, O., Kümmerer, D., Mader, I., Weiller, C., Klöppel, S., 2010. Early functional magnetic resonance imaging activations predict language outcome after stroke. Brain 133, 1252–1264. doi:10.1093/brain/awq021.

Sebastian, R., Schein, M.G., Davis, C., Gomez, Y., Newhart, M., Oishi, K., Hillis, A.E., 2014. Aphasia or Neglect after Thalamic Stroke: the Various Ways They may be Related to Cortical Hypoperfusion. Front Neurol 5, 231. doi:10.3389/fneur.2014.00231.

Stockert, A., Kümmerer, D., Saur, D., 2016. Insights into early language recovery: from basic principles to practical applications. Aphasiology 30, 517–541. doi:10.1080/02687038.2015.1119796.

Stockert, A., Wawrzyniak, M., Klingbeil, J., Wrede, K., Kümmerer, D., Hartwigsen, G., Kaller, C.P., Weiller, C., Saur, D., 2020. Dynamics of language reorganization after left temporo-parietal and frontal stroke. Brain 143, 844–861. doi:10.1093/brain/awaa023.

Vallar, G., Perani, D., Cappa, S.F., Messa, C., Lenzi, G.L., Fazio, F., 1988. Recovery from aphasia and neglect after subcortical stroke: neuropsychological and cerebral perfusion study. J. Neurol. Neurosurg. Psychiatr. 51, 1269–1276. doi:10.1136/jnnp.51.10.1269.

von Monakow, C., 1914. Die Lokalisation im Grosshirn und der Abbau der Funktion durch kortikale Herde. Bergmann, Wiesbaden, 1033 pp.

Wallesch, C.W., Johannsen-Horbach, H., Bartels, C., Herrmann, M., 1997. Mechanisms of and misconceptions about subcortical aphasia. Brain Lang 58, 436–458. doi:10.1006/brln.1997.1805, 403-9; discussion.

Wawrzyniak, M., Klingbeil, J., Zeller, D., Saur, D., Classen, J., 2018. The neuronal network involved in self-attribution of an artificial hand: a lesion network-symptom-mapping study. Neuroimage 166, 317–324. doi:10.1016/j.neuroimage.2017.11.011.

Weiller, C., Isensee, C., Rijntjes, M., Huber, W., Müller, S., Bier, D., Dutschka, K., Woods, R.P., Noth, J., Diener, H.C., 1995. Recovery from Wernicke's aphasia: a positron emission tomographic study. Ann. Neurol. 37, 723–732. doi:10.1002/ana.410370605.

Weiller, C., Willmes, K., Reiche, W., Thron, A., Isensee, C., Buell, U., Ringelstein, E.B., 1993. The case of aphasia or neglect after striatocapsular infarction. Brain 116 (Pt 6), 1509–1525. doi:10.1093/brain/116.6.1509.

Witte, O.W., Bidmon, H.J., Schiene, K., Redecker, C., Hagemann, G., 2000. Functional differentiation of multiple perilesional zones after focal cerebral ischemia. J. Cerebral Blood Flow Metabol. 20, 1149–1165. doi:10.1097/00004647-200008000-00001.

Xing, S., Lacey, E.H., Skipper-Kallal, L.M., Jiang, X., Harris-Love, M.L., Zeng, J., Turkeltaub, P.E., 2016. Right hemisphere grey matter structure and language outcomes in chronic left hemisphere stroke. Brain 139, 227–241. doi:10.1093/brain/awv323.

Yourganov, G., Fridriksson, J., Rorden, C., Gleichgerrcht, E., Bonilha, L., 2016. Multivariate connectome-based symptom mapping in post-stroke patients: networks supporting language and speech. J. Neurosci. 36, 6668–6679. doi:10.1523/JNEUROSCI.4396-15.2016.